pH Dependent Binding Energies of Broadly Neutralizing Antibodies

Scott P. Morton
Center for Computational Science
Middle Tennessee State University
Murfreesboro, TN, USA
0000-0002-3777-7089

Joshua L. Phillips
Department of Computer Science
Middle Tennessee State University
Murfreesboro, TN, USA
0000-0002-4619-6083

***Abstract*—Understanding how pH modulates underlying protein-protein interaction requires in-depth analysis across combinations of HIV proteins and broadly neutralizing antibodies (bnAbs). Traditional labs are not practical to screen all sequence variations and titrate of pH, highlighting the need to analyze such interactions theoretically. To fill this need, we generate homology models of predetermined HIV-1 gp120 in complex with bnAbs, through computational simulations to observe the binding energies as environmental pH varies. We compare simulation data to experimental data of the same structures at pH 5.5 and pH 7.4 specifically to present an 83.3% agreement between the two approaches to support the hypothesis that binding is stronger at lower pH. We then make observations of binding energy predictions across broad spectrum pH to provide insight into factors limiting the effectiveness of bnAbs *in vivo*. We conclude that theoretical models, and simulations involving them, provide data that closely mimic those of laboratory results.**

***Index Terms*—HIV, Env, gp120, CD4, electrostatics, binding, pH, mucosa**

I. Introduction

The human immunodeficiency virus (HIV) was identified in 1983 [1], [2] with research ensuing since that time in an attempt to produce a vaccine. HIV is typically transmitted in a mucosa pool during sexual intercourse when the gp120 protein subunit of the viral envelope (Env) makes contact with a CD4 receptor on host T-cell membranes. Interaction between the two molecules initiates binding and introduction of viral RNA to begin replication.

The challenge that scientists face is the overwhelming rate of evolutionary change HIV exhibits after introduction into the body. Additionally, clinical studies have shown that the largest population of HIV variants are not responsible for transmission of the infection from one host to another [3]–[6]. This fact introduces other challenges that leads researchers in the field to conclude that an effective vaccine requires a greater understanding of the mechanics involved with the infection process [7]–[10].

Research in the field has largely focused on broadly neutralizing antibodies (bnAbs) that target regions of gp120 at the CD4 binding site (CD4bs), V2-apex, V3-glycan regions and membrane-proximal external region (MPER) of sub unit protein gp41 [11]–[15]. Significant effort is focusing on CD4bs variants where high rates of neutralization occur; two such bnAbs, 3BNC117 and VRC01, have been the subject of studies showing movement towards a vaccine [16]–[20]. Efforts to improve potentiate have resulted in modified variants of bnAb 10E8 using hydrophobic or positively charged amino acids to present increased potency without diminishing functional breadth [16]. LaBranche et al. also provides encouraging results for wild types and engineered variants of CH235 that display increased potency [11].

Mutations in protein sequences can directly impact structural surface charges as demonstrated computationally [21]–[25]. Additionally, changes in surface electrostatics can impact structure sensitivity to changes in the surrounding environment. Indeed, physiological characteristics of the human body, namely pH, varies based on location and function; these changes in acidic content alter surface charge values [26] which can work in advantageous or adversarial ways when two proteins interact.

Here we apply a computational method of analyzing binding energies and the effect pH has on the interactions of bnAbs with gp120. We submit the hypothesis that *binding energies increase as pH increases numerically*, meaning that the energy required to bind two proteins together increases as pH rises. We compare the theoretical results against experimental results at pH 5.5 and pH 7.4 specifically. To translate the hypothesis in terms of laboratory results, we state that *neutralization decreases as pH increases numerically*; meaning that it is more difficult for bnAbs to bind with and neutralize gp120 as pH rises.

We then provide observations of theoretical data across pH in broad spectrum ranging from pH 3.0 to pH 9.0 in 0.1 increments. These data provide insight that is not observable in limited titrate that provides the ability to examine how the addition, removal, replacement or transposition of residues in gp120 and bnAb structures affects binding efficacy across a wide range of pH. Additionally, we provide binding energy results for the complex of gp120 and CD4 receptor proteins (CD4 is the target for gp120 during the infections process). This provides a way to compare the binding affinity of gp120/bnAb interactions to that of gp120/CD4.

978-1-6654-0126-5/21/$31.00 ©2021 IEEE

II. Materials and Methods

A. Protein Structures

Structures are from four separate lab experiments evaluating known antibody binding locations: CD4bs, V2/V3/Glycan, N332 Glycan, Glycan, MPER and Polyclonal. Eleven gp120 proteins were screened against fifteen bnAbs at pH 5.5 and pH 7.4. Species of gp120 evaluated are: 1056_10 (EU289186), 6101_1 (AY835434), 6535_3 (AY835438), CAAN_A2 (AY835452), PVO_4 (AY835444), RHPA_7 (AY835447), THRO_18 (AY835448), TRJO_58 (AY835450), TRO_11 (AY835445), WEAU_d15 (EU289202) and WITO_33 (AY835451). Species of bnAbs evaluated are: 10E8, 2F5, 2G12, 3BNC117, 4E10, B12, CH01, CH31, HIVIG-C, PG16, PG9, PGT121, PGT128, and VRC01. Combinations of bnAbs and gp120 will be referred to here as a *Complex*.

B. Neutralization assays

Neutralizing antibodies were measured with Env-pseudoyped viruses using TZM-bl cells as targets for infection essentially as described [27], [28] with minor modification. Briefly, TZM-bl cells were pre-seeded at a density of 8,000 cells/well in 96-well culture plates and incubated overnight at 37°C. In a separate plate, a pre-titrated dose of pseudovirus was incubated for 1 hr at 37°C with serial 3-fold dilutions of test sample in duplicate in a total volume of 150 μl of standard growth medium (DMEM, 10% fetal bovine serum, gentamicin 50 μg/ml, HEPES, pH 7.4) and the same growth medium (-HEPES) adjusted to pH 5.5 using 1N HCl. During this incubation period, all growth medium in the plates containing cells was replaced with 150 μl of either pH 7.4 or pH 5.5 growth medium containing 75 μg/ml DEAE dextran. After the incubation, the virus/sample mixtures were transferred to the cell plates. One set of control wells received cells + virus (virus control) and another set received cells only (background control). After 48 hours of incubation, 100 μl of cells was transferred to a 96-well black solid plate (Costar) for measurements of luminescence using the Britelite Luminescence Reporter Gene Assay System (PerkinElmer Life Sciences). Neutralization titers are the dilution (serum/plasma samples) or concentration (mAbs) at which relative luminescence units (RLU) are reduced by 50% compared to virus control wells after subtraction of background RLUs. Assay stocks of molecularly cloned Env-pseudotyped viruses will be prepared by transfection in 293T/17 cells (American Type Culture Collection) and titrated in TZM-bl cells as described [27], [28].

C. Computational Methods

The ESSC pipeline calculates the average charge across the solvent accessible surface (SAS) of the molecule being analyzed by determining all grid points containing SAS atoms using APBS [29], [30] data generated for the entire molecule. Binding energies are calculated using the free binding energy cycle provided by APBS. Complete details of the methods related to the electrostatic pipeline can be found in [21]–[26], [31].

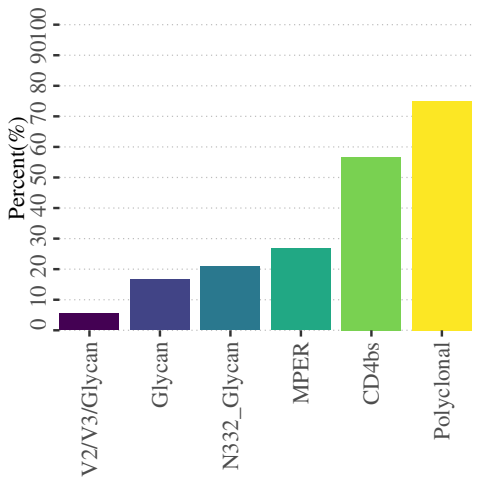

Fig. 1. Aggregation of experimental data grouped by binding location. Columns represent the percentage of entries where neutralization diminished as pH increases.

III. Results

A. Experimental Data

Lab experiments produce two hundred and four records of pH 5.5 and pH 7.4 pairs, seven bnAbs were not evaluated in experiment four. Some gp120 proteins (65535_3, TRO_11, WITO_33) were analyzed twice and CAAN_A2 was processed three times. For results that indicated neutralization resistance, for example the CD4bs cutoff is >25, we used the integer presented after the '>' symbol as the maximum value possible. Where results for each pair of pH 5.5 and pH 7.4 contained one entry indicating neutralization resistance, the comparison is considered legitimate to evaluate the hypothesis. Experimental results contain three records consisting of 'NA' and are presented here for completeness. Any pair containing 'NA' in one or both fields were not evaluated against the hypothesis or theoretical data.

We present Figures 1, 2, and 3 as analysis of experimental data in context of the hypothesis. Figure 1 is the aggregation of all experimental data in terms of each binding site. Figure 2 also is an aggregation of all experimental results in terms of gp120 and Figure 3 is in terms of bnAbs. Percentages indicate the ratio of complexes that agree with the hypothesis in all three figures.

We observe in Figure 1 that CD4bs and Polyclonal exceed 50% in terms of agreement with the hypothesis. All other binding locations are less than 30% agreement. In Figure 2, we observe that gp120's 6101_1, WEAU_d15, and 1056_10 are in agreement with the hypothesis at 50% or greater. Examining Figure 3 reveals that bnAbs CH31, 3BNC117, NIVIG-C, and VCCR01 are greater than 50% in agreement with the hypothesis.

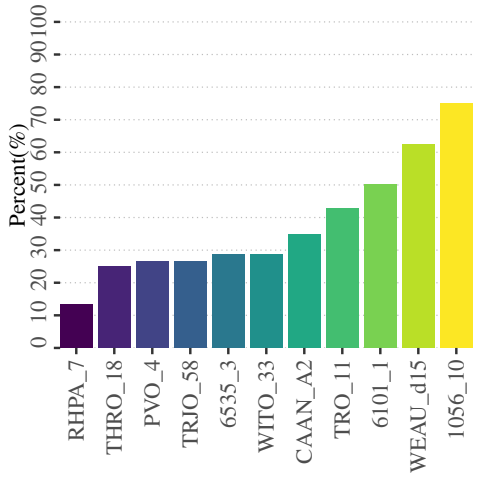

Fig. 2. Aggregation of all experimental data by gp120. Columns represent the percentage of entries where neutralization diminished as pH increases.

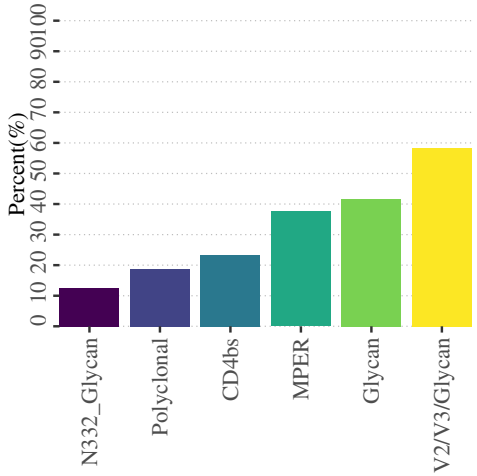

Fig. 4. Aggregation of experimental data grouped by binding location. Columns represent the percentage of entries detected as neutralization resistant.

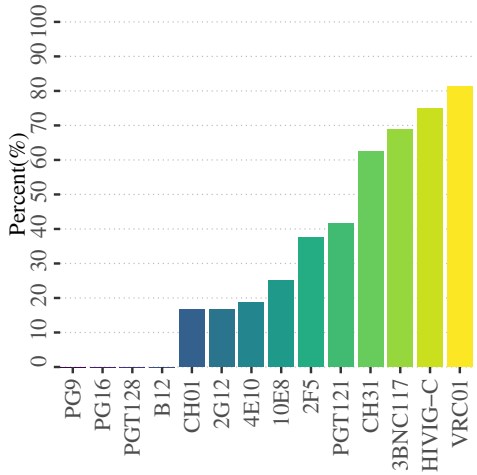

Fig. 3. Aggregation of all experimental data by bnAb. Columns represent the percentage of entries where neutralization diminished as pH increases.

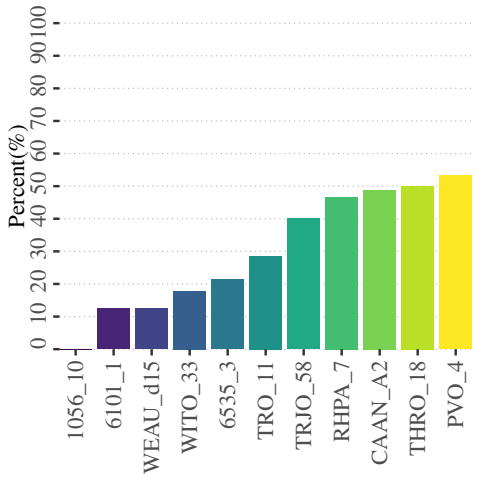

Fig. 5. Aggregation of experimental data grouped by gp120. Columns represent the percentage of entries detected as neutralization resistant.

The experimental data presents information that suggest neutralization resistance through formulation [27], [28]. Figures 4, 5, and 6 express the data in terms of neutralization resistance. Figure 4 is in terms of binding sites, Figure 5 is in terms of gp120 and Figure 6 expresses in terms of bnAbs. Percentages indicate the ratio of complexes that express neutralization resistance.

Inspection of Figure 4 reveals that the V2/V3/Glycan binding site has the highest neutralization resistance results. Examining Figure 5 provides indications that approximately 45% of gp120's analyzed have return 40% or greater neutralization resistant results. Figure 6 reveals that 50% of bnAbs analyzed present in excess of 40% neutralization resistance.

B. Theoretical Data

Limitations in available crystal structures restrict the computational pipeline to assessment of CD4bs at the theoretical level, but further studies could be performed on alternate binding targets when suitable structures become available. This fact provides a reduced set of bnAbs for theoretical analysis: 3BNC117, B12, CH31, and VRC01. All previously stated gp120 structures are analyzed. For presentation, theoretical data is normalized as follows:

$$x' = \frac{x - set_{min}}{set_{max} - set_{min}}, \tag{1}$$

Where x is the theoretical value, set_{min} is the minimum value of all theoretical data produced, set_{max} is the maximum value of all theoretical data produced, and x' is the normalized value returned.

We present theoretical data in similar fashion as experimental data where applicable. Theoretical data consists of a single binding site and, due to the number of results, prohibits deter-

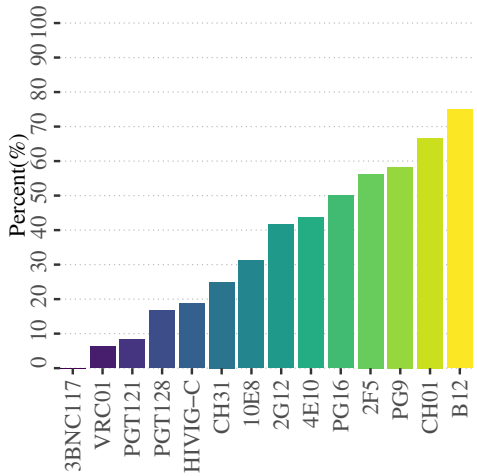

Fig. 6. Aggregation of experimental data grouped by bnAb. Columns represent the percentage of entries detected as neutralization resistant.

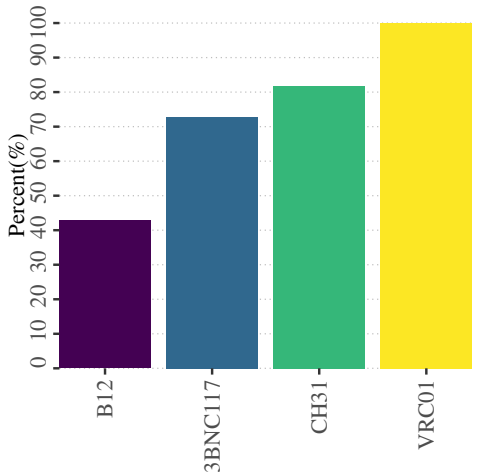

Fig. 8. Aggregation of theoretical data at pH 5.5 and pH 7.4 grouped by bnAb. Columns represent the percentage of entries where binding energy increases as pH increases.

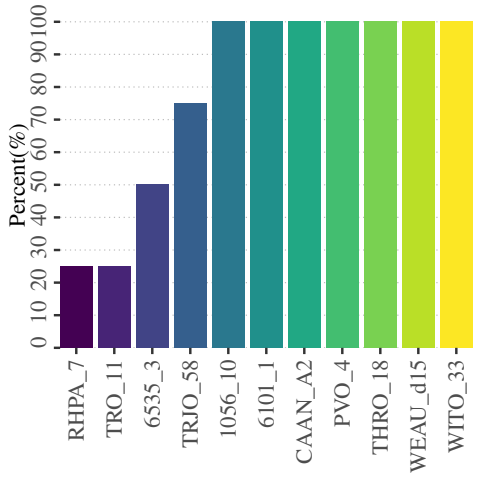

Fig. 7. Aggregation of theoretical data at pH 5.5 and pH 7.4 grouped by gp120. Columns represent the percentage of entries where binding energy increases as pH increases.

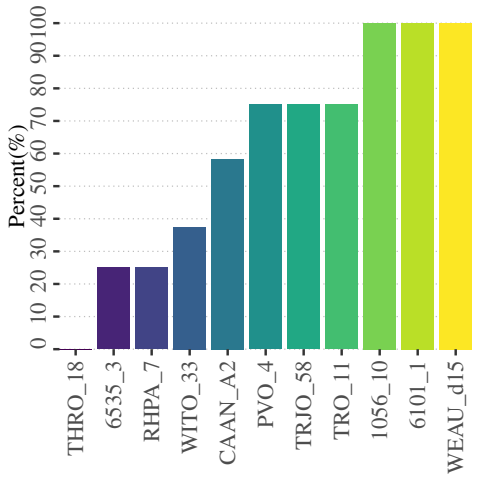

Fig. 9. Aggregation of experimental data at CD4bs grouped by gp120. Columns represent the percentage of entries neutralization diminished as pH increases.

mination of a cut off value that would suggest neutralization resistance in theory. These facts present two plots in terms of gp120 and bnAbs with the following explanations.

Figure 7 displays the percentages of complexes that agree with the hypothesis in terms of gp120. Figure 8 expresses results in terms of bnAbs, expressing the percentage of complexes that agree with the hypothesis.

Examining Figure 7 indicates that 81.8% of gp120s studied are 50% or greater in agreement with the hypothesis while 63.6% are 100% in agreement with the hypothesis. Figure 8 expresses 75% of bnAbs evaluated are in agreement with the hypothesis.

C. Comparing Results

To generally compare experimental results with theoretical results we produce Figures 9 and 10, which are aggregates of experimental results specifically at the CD4bs. Figure 9 displays 63.6% of gp120s agree with the hypothesis at greater than 50%, while Figure 10 shows that 75% of bnAbs display greater than 50% agreement with the hypothesis.

Comparing experimental results at the CD4bs by gp120 in Figure 9 with theoretical results in Figure 7 presents significant agreement between the two methods. Experimentally, we have 1056_10, 6101_1, and WEAU_d15 in complete agreement with theoretical counter parts. Experimental results for gp120s CAAN_A2, PVO_4, TRJO_58, and TRO_11 all exceeding 50% conformity with the hypothesis to suggest significant agreement with theoretical counter parts.

Comparing experimental results at the CD4bs for bnAbs in Figure 10 with theoretical results in Figure 8 also displays significant agreement between the two methods. With bnAb B12

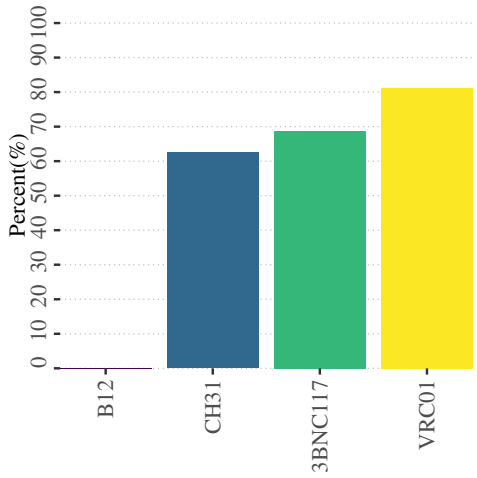

Fig. 10. Aggregation of experimental data at CD4bs grouped by bnAb. Columns represent the percentage of entries neutralization diminished as pH increases.

of Figure 10 dissenting from conformity with the hypothesis completely, all remaining bnAbs are in excess of 60% agreement with the hypothesis and therefore presenting significant concurrence with theoretical results shown in Figure 8.

Figure 11 is a detailed comparison of all lab results (top) to theoretical data (bottom). Duplicate complexes in experimentation are represented by the individual entry in theoretical data. To allow greater visual fidelity with the experimental data (top), the y-axis is constrained at 0 to16. The two sub-graphs utilize blue to represent pH 5.5 and red to indicate pH 7.4. Markers above each sub-graph indicate the following: $+/-$ represent the direction of change from low to high pH, 'R' represents resistance to neutralization in experimental data, 'N' indicates the presence of 'NA' in one or both fields of experimental results. The background color indicates agreement in reference to change in direction between theory and experiment using a green shade, disagreement using yellow shading and gray to indicate neutralization resistance or the presence of 'NA' in lab results. Complexes are noted as bnAb/gp120 along the horizontal axis. Scale is presented for completeness, however, scale is not considered in Figure 11 because theoretical results are the normalized values of electrostatic potential and experimental data is a percentage of change [27], [28].

These data indicate agreement between the two methods where lab results show increased resistance to neutralization at pH 7.4 and theoretical predictions indicate increased energy is required to bind the two proteins at pH 7.4. We remove any instance of neutralization resistance or 'NA' from calculations involving agreement for the following reasons: (1) We currently do not have a means to describe neutralization resistance in theoretical data, therefore, we cannot determine agreement, and (2) Results containing 'NA' are not comparable. As such, the two methods present 83.3% agreement.

D. Broad Spectrum Observations

In this section we make observations of broad spectrum data provided by theoretical predictions. Figure 12 shows four panels with binding patterns of the selected bnAbs: (A) 3BNC117, (B) B12, (C) CH31, and (D) VRC01 for the evaluated gp120 proteins. The red vertical bar is conservatively placed at the approximate point where unpredictable binding energies end, while the red shaded background predicts the functional range of each bnAb where the hypothesis is supported. Additionally, our data supports the hypothesis that *fluctuations in the starting pH and range of expected binding predictability controls breadth of effectiveness in vivo* as supported by [25], [26], [31] where gp120 has a higher affinity to bind at approximately pH 4.6.

Figure 12 shows wide variations in binding energies predicted computationally below pH 6.0 that may explain, in part, sporadic indicators of reduced neutralization in experimental data as pH increases. In the case of B12, the motif clearly explains rejection of the hypothesis for most Complexes; the binding energies are tightly related with a high peak at pH 5.5 where these values are generally greater than the those returned at pH 7.4. B12 is also observed to be centered vertically across Complexes more so than others. A detailed analysis of B12 versus other strains of bnAbs would be required to properly understand this phenomenon.

Mascola et al. compiled data of various site functional bnAbs including breadth and potency specific information [10]. Our observations mostly agree with Mascola et al. in terms of breadth and potency versus starting pH and functional range as shown by Figure 12 and expressed respectively in the following:

- 3BNC117 has good breadth with good potency (+++, +++) and good starting pH (5.9) with good range of 2.6 (5.9 - 8.5)
- B12 has low breadth with moderate potency (+, ++) and high starting pH (6.2) with good range of 2.7 (6.2 - 8.9)
- VRC-CH30-34 lineages have good breadth with good potency (+++, +++) and high starting pH with low range 2.2 (6.3–8.5)
- VRC01-03 lineages have wide breadth with good potency (++++, +++) and low starting pH (5.6) with wide range 2.9 (5.6–8.5)

Additionally, we perform the same processing utilizing the T-cell CD4 receptor sequence sourced from NCBI Genbank accession number 1RZK_C.. This bridges the analysis of immune response with that of the infection process by comparing the binding energy motif of proteins presented in defense, as in Figure 12, to those encountered during infections, as shown in Figure 13. As can be observed, a large discrepancy exists between the hypothesized functional range of the studied gp120/bnAb complexes versus that of gp120/CD4.

IV. Conclusions

We established a foundation to study binding energies of various molecular structures in computational simulations.

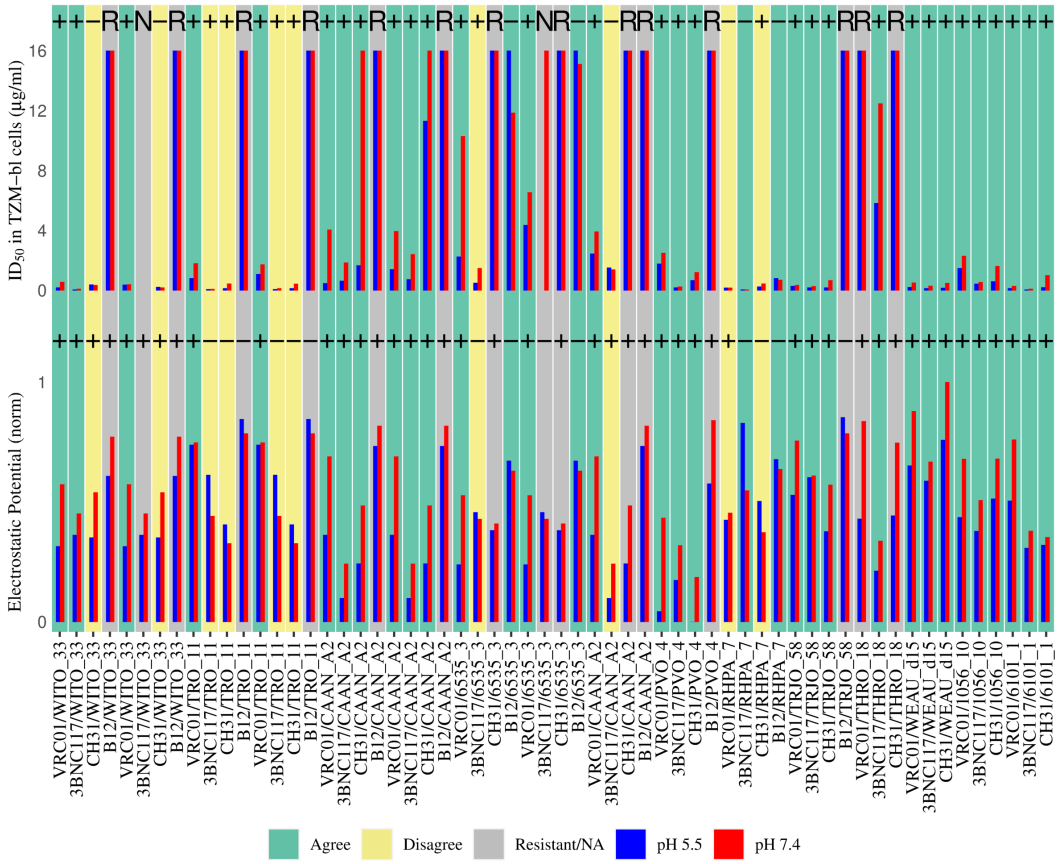

Fig. 11. Graph showing the comparison of lab results (top) to theoretical data (bottom) with blue representing pH 5.5 and red indicating pH 7.4. Markers indicate the following: $+/-$ represent the direction of change from low to high pH, 'R' represents resistance to neutralization in experimental data, 'N' indicates an 'NA' is present in one or more fields for experimental data. The background color indicates agreement in reference to change in direction between theory and experiment using a green shade, disagreement using yellow shading and gray to indicate neutralization resistance or the presence of 'NA' in lab data. Complexes are noted as bnAb/gp120 along the horizontal axis.

Points of interest across gp120 provide a broad range of opportunities to evaluate the theoretical approach, however, we have focused this research on those instances involving bnAbs which bind gp120 at CD4bs. The results are complimented by laboratory experimentation and indicate an 83.3% agreement between the two approaches. Additionally, our theoretical results indicate that pH is a major component in binding efficacy of bnAbs and gp120 at the CD4 binding site. Our results and observations agree with past research in this field where an observable range of predictable outcomes indicates a functional range in bnAbs that coincides with potency and breadth of wild type bnAbs. These predictions are across a pH range that encompasses the human physiological pH range and therefore provides the potential to make observations in solvents that would likely denature proteins in ways that are not observable in natural environments.

Additionally, Figure 12 provides great insight into the need to perform broad spectrum analysis to determine the effect pH has on binding efficacy. Undulations in binding energy below pH 6.0 for most bnAbs would cause a contradiction of naturally occurring changes, as can be observed when comparing experimental data of Figure11 (top) to theoretical data of Figure 12. The selection of pH values used for experimental purposes barely agrees with hypothesis' presented here and had other values been chosen as the lower pH concentration, the results may have contrasted theoretical predictions to the point of contention.

We further conclude that clearly, bnAbs dictate binding potential motif of the complexes across varying pH levels as is observed in Figure 12. However, the studied bnAbs lack the functional capacity to bind with gp120 across the observed pH range in comparison to that of gp120 to CD4 binding. These data suggest that ranges of physiological pH exist where gp120 can continue to infect new cells uninhibited by bnAbs to effectively 'escape' the immune system response.

Additionally, we submit that further studies are required to identify where each bnAb denatures at the extremes of pH to provide further evidence supporting the hypothesis' presented here for consideration.

ACKNOWLEDGMENT

The authors would like to thank Dr. Bette M. Korber of the Theoretical Biology and Biophysics (T-6) Lab at Los Alamos National Laboratory for the suggested variants of

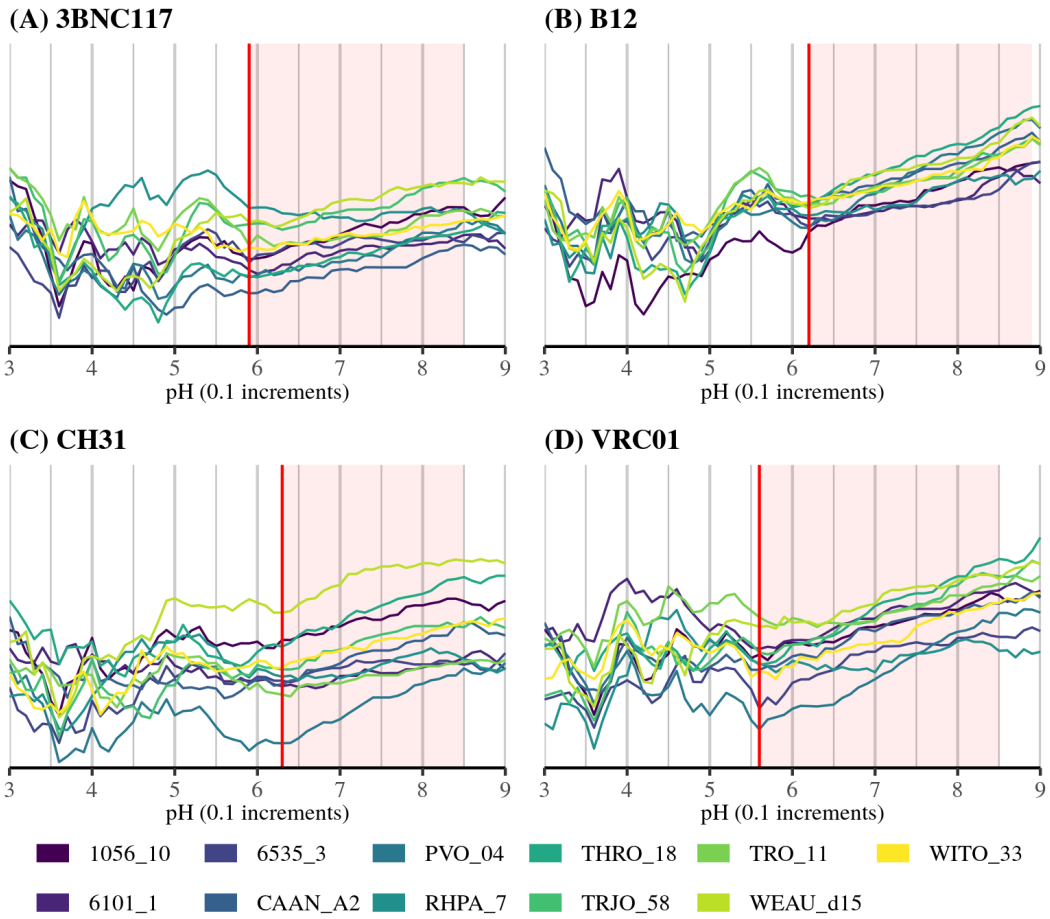

Fig. 12. Broad spectrum binding energy motifs of bnAbs (A) 3BNC117, (B) B12, (C) CH31, (D) VRC01 displaying the affinity each has binding to the eleven gp120 proteins analyzed. The red vertical bar is conservatively placed at the approximate pH value where, to the right, outcomes become predictable in their positive movement as pH rises. The shaded background indicates the functional range of predictable activity. Data is the normalized mean of electrostatic potential for ten models.

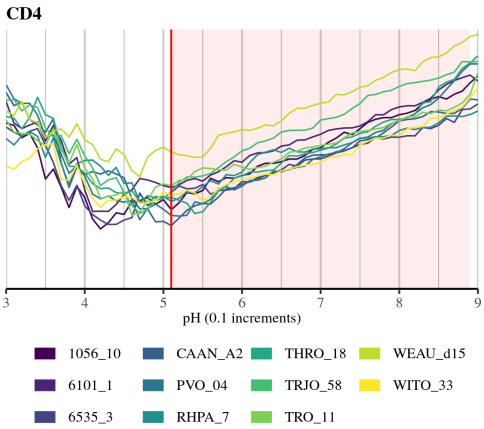

Fig. 13. Broad spectrum binding energy motifs of gp120 with CD4. The red vertical bar is conservatively placed at the approximate pH value where, to the right, outcomes become predictable in their positive movement as pH rises. The shaded background indicates the functional range of predictable activity. Data is the normalized mean of electrostatic potential for ten models.

gp120 and bnAb for the experimental data in addition to the feedback and suggestions on the content provided here. We would also thank Dr. Miroslawa Bilska and Dr. David C. Montefiori of the Laboratory for AIDS Vaccine Research and Development in the Department of Surgery, Division of Surgical Sciences, Duke University Medical Center, Durham, NC for the exceptional work performed in the production of experimental data that made this research possible.

References

[1] F. Barre-Sinoussi, J. Chermann, F. Rey, M. Nugeyre, S. Chamaret, J. Gruest, C. Dauguet, C. Axler-Blin, F. Vezinet-Brun, C. Rouzioux, W. Rozenbaum, and L. Montagnier, "Isolation of a T-lymphotropic retrovirus from a patient at risk for acquired immune deficiency syndrome (AIDS)," *Science*, vol. 220, no. 4599, pp. 868–871, may 1983.

[2] R. Gallo, P. Sarin, E. Gelmann, M. Robert-Guroff, E. Richardson, V. Kalyanaraman, D. Mann, G. Sidhu, R. Stahl, S. Zolla-Pazner, J. Leibowitch, and M. Popovic, "Isolation of human T-cell leukemia virus in acquired immune deficiency syndrome (AIDS)," *Science*, vol. 220, no. 4599, pp. 865–867, may 1983.

[3] D. I. Boeras, P. T. Hraber, M. Hurlston, T. Evans-Strickfaden, T. Bhattacharya, E. E. Giorgi, J. Mulenga, E. Karita, B. T. Korber, S. Allen, C. E. Hart, C. a. Derdeyn, and E. Hunter, "Role of donor genital tract HIV-1 diversity in the transmission bottleneck," *Proceedings*

of the National Academy of Sciences, vol. 108, no. 46, pp. E1156–E1163, nov 2011.

[4] C. C. A. Derdeyn, J. M. J. Decker, F. Bibollet-Ruche, J. L. J. Mokili, M. Muldoon, S. A. S. Denham, M. L. M. Heil, F. Kasolo, R. Musonda, B. B. H. Hahn, G. M. G. Shaw, B. T. Korber, S. Allen, and E. Hunter, "Envelope-constrained neutralization-sensitive HIV-1 after heterosexual transmission," *Science*, vol. 303, no. 5666, pp. 2019–2022, mar 2004.

[5] R. E. Haaland, P. A. Hawkins, J. Salazar-Gonzalez, A. Johnson, A. Tichacek, E. Karita, O. Manigart, J. Mulenga, B. F. Keele, G. M. Shaw, B. H. Hahn, S. A. Allen, C. A. Derdeyn, and E. Hunter, "Inflammatory genital infections mitigate a severe genetic bottleneck in heterosexual transmission of subtype A and C HIV-1." *Public Library of Science Pathogens*, vol. 5, no. 1, p. e1000274, jan 2009.

[6] B. F. Keele, E. E. Giorgi, J. F. Salazar-Gonzalez, J. M. Decker, K. T. Pham, M. G. Salazar, C. Sun, T. Grayson, S. Wang, H. Li, X. Wei, C. Jiang, J. L. Kirchherr, F. Gao, J. A. Anderson, L.-H. Ping, R. Swanstrom, G. D. Tomaras, W. A. Blattner, P. A. Goepfert, J. M. Kilby, M. S. Saag, E. L. Delwart, M. P. Busch, M. S. Cohen, D. C. Montefiori, B. F. Haynes, B. Gaschen, G. S. Athreya, H. Y. Lee, N. Wood, C. Seoighe, A. S. Perelson, T. Bhattacharya, B. T. Korber, B. H. Hahn, and G. M. Shaw, "Identification and characterization of transmitted and early founder virus envelopes in primary HIV-1 infection." *Proceedings of the National Academy of Sciences of the United States of America*, vol. 105, no. 21, pp. 7552–7557, may 2008.

[7] B. F. Haynes and J. R. Mascola, "The quest for an antibody-based HIV vaccine," *Immunological Reviews*, vol. 275, no. 1, pp. 5–10, jan 2017.

[8] A. S. Fauci, "An HIV vaccine," *The Journal of the American Medical Association*, vol. 316, no. 2, p. 143, jul 2016.

[9] B. F. Haynes, G. M. Shaw, B. Korber, G. Kelsoe, J. Sodroski, B. H. Hahn, P. Borrow, and A. J. McMichael, "HIV-Host interactions: Implications for vaccine design," *Cell Host & Microbe*, vol. 19, no. 3, pp. 292–303, mar 2016.

[10] J. R. Mascola and B. F. Haynes, "HIV-1 neutralizing antibodies: understanding nature's pathways," *Immunological Reviews*, vol. 254, no. 1, pp. 225–244, jul 2013.

[11] C. C. LaBranche, R. Henderson, A. Hsu, S. Behrens, X. Chen, T. Zhou, K. Wiehe, K. O. Saunders, S. M. Alam, M. Bonsignori, M. J. Borgnia, Q. J. Sattentau, A. Eaton, K. Greene, H. Gao, H. X. Liao, W. B. Williams, J. Peacock, H. Tang, L. G. Perez, R. J. Edwards, T. B. Kepler, B. T. Korber, P. D. Kwong, J. R. Mascola, P. Acharya, B. F. Haynes, and D. C. Montefiori, "Neutralization-guided design of HIV-1 envelope trimers with high affinity for the unmutated common ancestor of CH235 lineage CD4bs broadly neutralizing antibodies," *Public Library of Science Pathogens*, vol. 15, no. 9, p. e1008026, sep 2019.

[12] P. D. Kwong, J. R. Mascola, and G. J. Nabel, "Broadly neutralizing antibodies and the search for an HIV-1 vaccine: the end of the beginning," *Nature Reviews Immunology*, vol. 13, no. 9, pp. 693–701, sep 2013.

[13] R. Wyatt, "The HIV-1 envelope glycoproteins: fusogens, antigens, and immunogens," *Science*, vol. 280, no. 5371, pp. 1884–1888, jun 1998.

[14] R. Pantophlet and D. R. Burton, "GP120: Target for neutralizing HIV-1 antibodies," *Annual Review of Immunology*, vol. 24, no. 1, pp. 739–769, apr 2006.

[15] J. Overbaugh and L. Morris, "The antibody response against HIV-1," *Cold Spring Harbor Perspectives in Medicine*, vol. 2, no. 1, pp. a007 039–a007 039, jan 2012.

[16] Y. D. Kwon, G.-Y. Chuang, B. Zhang, R. T. Bailer, N. A. Doria-Rose, T. S. Gindin, B. Lin, M. K. Louder, K. McKee, S. O'Dell, A. Pegu, S. D. Schmidt, M. Asokan, X. Chen, M. Choe, I. S. Georgiev, V. Jin, M. Pancera, R. Rawi, K. Wang, R. Chaudhuri, L. A. Kueltzo, S. D. Manceva, J.-P. Todd, D. G. Scorpio, M. Kim, E. L. Reinherz, K. Wagh, B. M. Korber, M. Connors, L. Shapiro, J. R. Mascola, and P. D. Kwong, "Surface-matrix screening identifies semi-specific interactions that improve potency of a near pan-reactive HIV-1-neutralizing antibody," *Cell Reports*, vol. 22, no. 7, pp. 1798–1809, feb 2018.

[17] K. J. Bar, M. C. Sneller, L. J. Harrison, J. S. Justement, E. T. Overton, M. E. Petrone, D. B. Salantes, C. A. Seamon, B. Scheinfeld, R. W. Kwan, G. H. Learn, M. A. Proschan, E. F. Kreider, J. Blazkova, M. Bardsley, E. W. Refsland, M. Messer, K. E. Clarridge, N. B. Tustin, P. J. Madden, K. Oden, S. J. O'Dell, B. Jarocki, A. R. Shiakolas, R. L. Tressler, N. A. Doria-Rose, R. T. Bailer, J. E. Ledgerwood, E. V. Capparelli, R. M. Lynch, B. S. Graham, S. Moir, R. A. Koup, J. R. Mascola, J. A. Hoxie, A. S. Fauci, P. Tebas, and T.-W. Chun, "Effect of HIV antibody VRC01 on viral rebound after treatment interruption," *New England Journal of Medicine*, vol. 375, no. 21, pp. 2037–2050, nov 2016.

[18] M. Caskey, F. Klein, J. C. C. Lorenzi, M. S. Seaman, A. P. West, N. Buckley, G. Kremer, L. Nogueira, M. Braunschweig, J. F. Scheid, J. A. Horwitz, I. Shimeliovich, S. Ben-Avraham, M. Witmer-Pack, M. Platten, C. Lehmann, L. A. Burke, T. Hawthorne, R. J. Gorelick, B. D. Walker, T. Keler, R. M. Gulick, G. Fätkenheuer, S. J. Schlesinger, and M. C. Nussenzweig, "Viraemia suppressed in HIV-1-infected humans by broadly neutralizing antibody 3BNC117," *Nature*, vol. 522, no. 7557, pp. 487–491, jun 2015.

[19] J. F. Scheid, J. A. Horwitz, Y. Bar-On, E. F. Kreider, C.-L. Lu, J. C. C. Lorenzi, A. Feldmann, M. Braunschweig, L. Nogueira, T. Oliveira, I. Shimeliovich, R. Patel, L. Burke, Y. Z. Cohen, S. Hadrigan, A. Settler, M. Witmer-Pack, A. P. West, B. Juelg, T. Keler, T. Hawthorne, B. Zingman, R. M. Gulick, N. Pfeifer, G. H. Learn, M. S. Seaman, P. J. Bjorkman, F. Klein, S. J. Schlesinger, B. D. Walker, B. H. Hahn, M. C. Nussenzweig, and M. Caskey, "HIV-1 antibody 3BNC117 suppresses viral rebound in humans during treatment interruption," *Nature*, vol. 535, no. 7613, pp. 556–560, jul 2016.

[20] T. Schoofs, F. Klein, M. Braunschweig, E. F. Kreider, A. Feldmann, L. Nogueira, T. Oliveira, J. C. C. Lorenzi, E. H. Parrish, G. H. Learn, A. P. West, P. J. Bjorkman, S. J. Schlesinger, M. S. Seaman, J. Czartoski, M. J. McElrath, N. Pfeifer, B. H. Hahn, M. Caskey, and M. C. Nussenzweig, "HIV-1 therapy with monoclonal antibody 3BNC117 elicits host immune responses against HIV-1," *Science*, vol. 352, no. 6288, pp. 997–1001, may 2016.

[21] J. Howton, "A computational electrostratic modeling pipeline for comparing pH-dependent gp120-CD4 interactions in founder and chronic HIV strains," Murfreesboro, TN, 2017.

[22] J. Howton and J. L. Phillips, "Computational modeling of pH-dependent gp120-CD4 interactions in founder and chronic HIV strains," in *Proceedings of the 8th ACM International Conference on Bioinformatics, Computational Biology,and Health Informatics - ACM-BCB '17*. Boston, MA, USA: ACM Press, 2017, pp. 644–649.

[23] S. P. Morton, J. Howton, and J. L. Phillips, "Sub-Class differences of pH-dependent HIV gp120-CD4 interactions," in *Proceedings of the 2018 ACM International Conference on Bioinformatics, Computational Biology, and Health Informatics - BCB '18*. New York, New York, USA: ACM Press, 2018, pp. 663–668.

[24] S. P. Morton, J. B. Phillips, and J. L. Phillips, "The molecular basis of pH-modulated HIV gp120 binding revealed," *Evolutionary Bioinformatics*, vol. 15, p. 117693431983130, jan 2019.

[25] S. P. Morton, "Methods of Electrostatic Analysis for Biomolecular Structures," *http://dissertations.umi.com/mtsu:11343*, 2020. [Online]. Available: https://jewlscholar.mtsu.edu/handle/mtsu/6299

[26] D. J. Stieh, J. L. Phillips, P. M. Rogers, D. F. King, G. C. Cianci, S. A. Jeffs, S. Gnanakaran, and R. J. Shattock, "Dynamic electrophoretic fingerprinting of the HIV-1 envelope glycoprotein," *Retrovirology*, vol. 10, no. 1, p. 33, 2013.

[27] D. C. Montefiori, "Measuring HIV neutralization in a luciferase reporter gene assay," in *HIV Protocols: Second Edition, Methods in Molecular Virology*. Humana Press, 2009, pp. 395–405.

[28] M. Li, F. Gao, J. R. Mascola, L. Stamatatos, V. R. Polonis, M. Koutsoukos, G. Voss, P. Goepfert, P. Gilbert, K. M. Greene, M. Bilska, D. L. Kothe, J. F. Salazar-Gonzalez, X. Wei, J. M. Decker, B. H. Hahn, and D. C. Montefiori, "Human immunodeficiency virus type 1 env clones from acute and early subtype B infections for standardized assessments of vaccine-elicited neutralizing antibodies." *Journal of Virology*, vol. 79, no. 16, pp. 10 108–25, aug 2005.

[29] N. A. Baker, D. Sept, S. Joseph, M. J. Holst, and J. A. McCammon, "Electrostatics of nanosystems: application to microtubules and the ribosome." *Proceedings of the National Academy of Sciences of the United States of America*, vol. 98, no. 18, pp. 10 037–10 041, aug 2001.

[30] E. Jurrus, D. Engel, K. Star, K. Monson, J. Brandi, L. E. Felberg, D. H. Brookes, L. Wilson, J. Chen, K. Liles, M. Chun, P. Li, D. W. Gohara, T. Dolinsky, R. Konecny, D. R. Koes, J. E. Nielsen, T. Head-Gordon, W. Geng, R. Krasny, G.-W. Wei, M. J. Holst, J. A. McCammon, and N. A. Baker, "Improvements to the APBS biomolecular solvation software suite," *Protein Science*, vol. 27, no. 1, pp. 112–128, jan 2018.

[31] S. P. Morton, J. B. Phillips, and J. L. Phillips, "High-throughput structural modeling of the HIV transmission bottleneck," in *Proceedings of the 2017 IEEE International Conference on Bioinformatics and Biomedicine - BIBM-HPCB '17*, vol. 2017-Janua. Kansas City, MO, USA: IEEE Press, 2017.